Research Article | Vol. 32, No. 8 / 8 Apr 2024 / Optics Express 13166
Optics EXPRESS

Kinetics of pair-induced quenching in holmium-doped optical fibers

André Wean Edvardsen[1,2,*] and Lars Grønmark Holmen[1]

[1]Norwegian Defence Research Establishment (FFI), Kjeller NO-2027, Norway
[2]Department of Technology Systems, University of Oslo, Kjeller NO-2027, Norway
[*]andre-wean.edvardsen@ffi.no

Abstract: We present a study of the dynamics of the rapid energy transfer upconversion that occurs within pairs or clusters of holmium ions, commonly referred to as pair-induced quenching. The lifetime of excited holmium ion pairs is determined to be around 0.4 µs from time-resolved fluorescence measurements. We develop a rate equation model that incorporates this lifetime and evaluate numerically and experimentally the consequences this finite intra-cluster upconversion rate has on the performance of a nanosecond-pulsed Ho-doped fiber amplifier. We demonstrate a significant improvement in efficiency by utilizing pulsed pumping on a timescale shorter than the measured excited ion pair lifetime.

1. Introduction

High-power fiber lasers operating in the 2 µm spectral regime are attractive for applications in areas such as remote sensing, materials processing, medicine, and defense [1]. Holmium-doped fiber sources can operate at wavelengths slightly longer than 2.1 µm, which is especially attractive because of the atmospheric transmission windows beyond 2.1 µm. Furthermore, Ho-doped fiber amplifiers are well-suited as pump sources for nonlinear frequency conversion to the mid-IR [2].

State-of-the-art Ho-doped fibers with relatively low holmium concentrations have been demonstrated to achieve very high slope efficiencies, reaching ~93% of the quantum defect limit in simple continuous wave (CW) oscillator setups [3]. However, Ho-doped fibers suitable for *pulsed* operation at high peak power have very different design requirements, such as short fiber lengths and large mode areas needed to suppress detrimental nonlinear effects. High Ho concentration is needed to achieve high gain and sufficient pump absorption over a short length, and pulsed amplifiers built from such fibers reported to date have performed significantly below the quantum defect limit. For example, a high repetition rate 2.1 µm amplifier with relatively long pulses of 322 ns reported a slope efficiency of ~50% w.r.t. 1980 nm pump light [4]. A different amplifier that was built using the same gain fiber was optimized for generating high peak power pulses of 10 ns duration. This amplifier operated at a much higher gain and achieved only 26% slope efficiency w.r.t. 1950 nm pump light [2].

Several studies have identified the process called *pair-induced quenching* (PIQ) as the leading cause of this lower-than-expected slope efficiency [2,5,–7]. PIQ is a rapid upconversion-related energy transfer process between two excited Ho ions within pairs or larger clusters of Ho ions in very close vicinity. The net outcome of the process is the relaxation of one of the two excited ions to the ground state, which reduces the gain and efficiency of an amplifier. To date, reported studies of PIQ in Ho-doped fibers have all assumed the PIQ interaction to be instantaneous [2,5,–7]. This approximation may be justified for amplifiers that operate in the CW regime but becomes questionable when considering, for example, pulsed amplifiers that operate with pulse widths comparable to or shorter than the interaction time characteristic of PIQ. To the best of our knowledge, no studies of the PIQ interaction dynamics have yet been reported for Ho-doped fibers. Therefore, the temporal regimes where the dynamics must be accounted for have not yet

#521512 https://doi.org/10.1364/OE.521512
Journal © 2024 Received 14 Feb 2024; revised 14 Mar 2024; accepted 14 Mar 2024; published 25 Mar 2024

Optics EXPRESS

been identified despite such knowledge being essential for correctly understanding and modeling pulsed amplifiers. For reference, in contrast to Ho-doped fibers, the fast kinetics of intra-cluster energy transfer processes have been experimentally studied for erbium-doped fibers [8,–11], and the lifetime of excited erbium ion pairs was reported to be 50 ns [10].

This paper presents an experimental and numerical study of the intra-cluster energy transfer dynamics in Ho-doped fibers. Time-resolved fluorescence measurements are done to determine, for the first time, the lifetime of excited Ho ion pairs. The dependence of the excited pair lifetime on parameters such as doping concentration and core composition is studied by measuring several different fibers. Our measurements reveal a relatively long excited pair lifetime, and we consider how this influences measurements of non-saturable absorption, arguably the most commonly used tool for characterizing PIQ. Furthermore, we study the practical impact of PIQ on a high-power nanosecond-pulsed Ho-doped fiber amplifier. We demonstrate that the efficiency is significantly improved by utilizing pulsed pumping compared to CW pumping and explain this result from the acquired understanding of the PIQ interaction dynamics.

Additionally, we present a numerical rate equation model for Ho-doped fiber amplifiers that accounts for dynamic aspects of PIQ by incorporating the lifetime of Ho ion pairs. This model forms a numerical framework for simulating and understanding pulsed amplifiers operating on timescales of comparable magnitude to the measured excited pair lifetime. The ability of our model to recreate the experimental findings of this work is assessed throughout the paper.

2. Upconversion and pair-induced quenching in holmium-doped fibers

An energy level diagram of the four lowest energy manifolds of Ho^{3+} in silica is shown in Fig. 1. The figure includes the most relevant energy transitions for in-band pumped Ho-doped fiber amplifiers, such as 1.95 µm pump absorption ($^5I_8 \rightarrow {}^5I_7$), stimulated emission at 2.1 µm ($^5I_7 \rightarrow {}^5I_8$) and non-radiative decay. The radiative transition $^5I_6 \rightarrow {}^5I_8$ is usually insignificant for in-band pumped Ho-doped amplifiers but will be used in Sec. 4.1 to probe the dynamics of the final energy transition shown in the figure; *energy transfer upconversion* (ETU). ETU is a cooperative ion-ion interaction between two excited ions in close proximity, induced by electric multipolar interactions. It starts with two Ho ions in the excited state $^5I_7$, of which one is demoted to the ground state ($^5I_8$) and the other is promoted to either the state $^5I_6$ or $^5I_5$. We refer to the first possibility ($^5I_7, {}^5I_7 \rightarrow {}^5I_8, {}^5I_6$) as ETU1 and to the second ($^5I_7, {}^5I_7 \rightarrow {}^5I_8, {}^5I_5$) as ETU2. Because of the short lifetime of $^5I_5$ (22 ns [12]), ions excited through ETU2 rapidly relax to $^5I_6$, from which further relaxation occurs shortly after (1.4 µs [12]) to the metastable upper laser level $^5I_7$ (lifetime ~1 ms [13]). Hence, the net outcome of ETU is that only one of the two initially excited ions remains in the upper laser level. As discussed by Jackson [12], the exothermic process ETU1 is much more likely to occur than the endothermic process ETU2. Considering also the short lifetime of $^5I_5$, it is justified to consider the two ETU processes collectively as purely ETU1.

It is common to distinguish between two types of upconversion in the context of PIQ [11]; *homogeneous upconversion* and *inhomogeneous upconversion*. Homogeneous upconversion is associated with the ETU interaction averaged over all interionic distances for ions assumed to be distributed *randomly* in the host. In the dipole-dipole approximation, the upconversion rate is proportional to $1/R^6$ [11], where R is the ion-ion separation. In this description, the rate of homogeneous upconversion is sensitive to doping concentration, owing to the fact that the separation between Ho ions decreases with increasing population densities. Conversely, inhomogeneous upconversion is associated with the ETU interaction between ions residing in clusters. This intra-cluster ETU process is very rapid due to the short ion separation and is much faster than homogeneous upconversion. Since the effect of inhomogeneous upconversion is the rapid loss of one excited ion, it is often referred to as pair-induced quenching. One notable difference from homogeneous upconversion is that intra-cluster ETU can be described with a

Optics EXPRESS

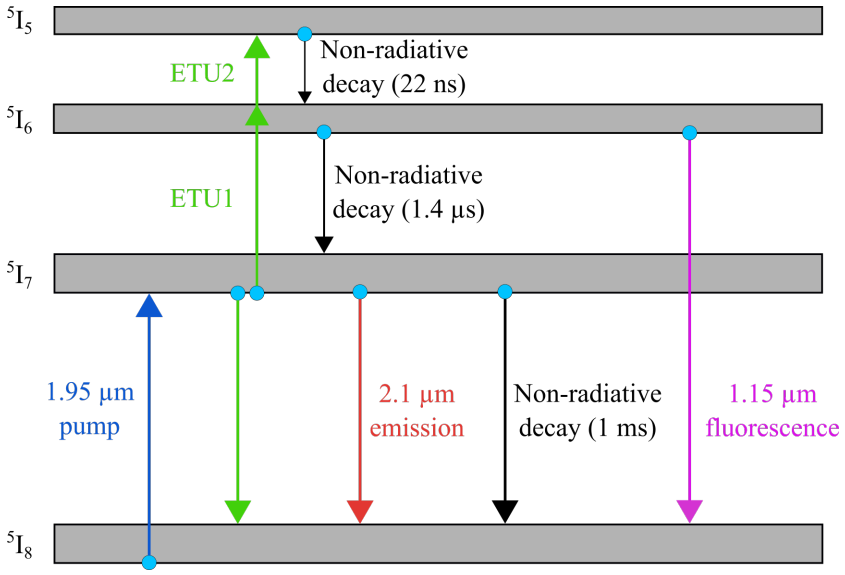

Fig. 1. Energy level diagram of the four lowest lying energy manifolds of Ho^{3+} in silica with the most relevant energy transitions indicated.

single rate independent of the doping concentration. This is because a pair or cluster acts as a distinct entity where the fixed ion separation results in a common interaction rate for all clusters. In this situation, it can be natural to think of the process in terms of a characteristic *lifetime* of the state where both ions in a pair are excited. In the following section, we develop a rate equation model where we incorporate such a lifetime to capture the dynamic aspects of inhomogeneous upconversion in Ho-doped optical fibers.

3. Rate equation model incorporating pair-induced quenching

A common method of incorporating the effects of pair-induced quenching in numerical models of fiber lasers and amplifiers is to divide the active ions into two species: non-clustered/single ions and clustered ions. In an actual optical fiber, the active ions will reside in clusters of different sizes, but in numerical models, the clusters are usually assumed to be in their simplest form: a pair. This method has been extensively utilized in numerical models of erbium-doped fiber amplifiers [8,11,14,15], and more recently for Ho-doped fiber amplifiers [2,5–7]. These models assume that the upconversion between ions within a pair occurs instantaneously. This assumption is reasonable when considering amplifiers operating in the CW regime but is expected to fail for amplifiers operating with pulse widths comparable to the energy transfer rates characteristic of PIQ.

The rate equation model we present here resembles closely that reported by Wang et al. [5,6], with the key difference that the rate of PIQ is not assumed to be infinitely fast. Instead, we present a dynamic model with detailed tracking of the various combinations of states an ion pair can have. The single ions can occupy the states $^5I_8$, $^5I_7$ and $^5I_6$, and the population densities of these states are denoted $N_0 - N_2$, as shown in Fig. 2(a). As discussed in Sec. 2, we assume that only the upconversion of type ETU1 occurs. Hence, the state $^5I_5$ is not considered. The combinations of states an ion pair can occupy are shown in Fig. 2(b) with population densities denoted $N_3 - N_7$. It is noted that a pair state where both ions occupy $^5I_6$ is excluded since it cannot be reached through the energy transfer mechanisms considered in this model. The upconversion rate of ion

Optics EXPRESS

pairs is expressed as $W_{\text{pair}} = 1/\tau_{\text{pair}}$, where τ_{pair} is the lifetime of excited ion pairs, in essence, state N_5 in Fig. 2(b). Following the convention from literature on PIQ [2,5–7,10,11], we denote the ratio of ions residing in pairs as $2k$. Thus, the concentration of ion pairs is kN_{Ho} and the concentration of single ions is $(1-2k)N_{\text{Ho}}$, where N_{Ho} is the doping concentration in units of ions/m^3.

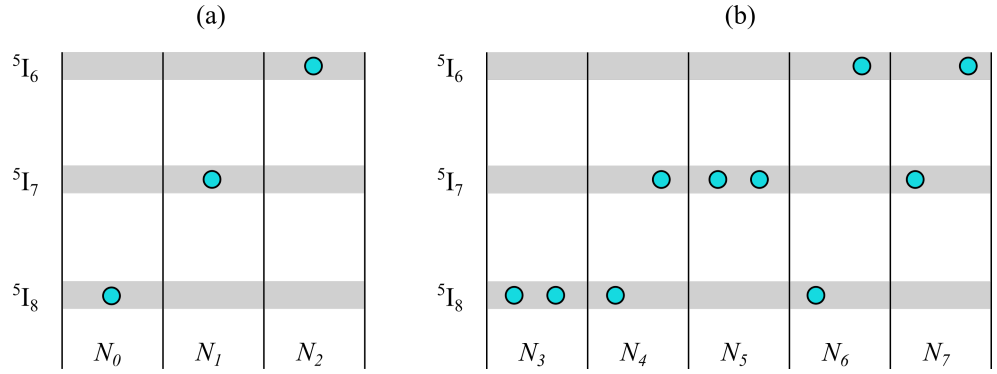

Fig. 2. The possible states that (a) single/non-clustered ions and (b) ion pairs can occupy.

The rate equations governing the population densities of the single ion states are

$$\frac{dN_0(z,t)}{dt} = W_{11}N_1(z,t)^2 + (W_{10} + W_{10}^{\text{p}} + W_{10}^{\text{s}})N_1(z,t) + W_{20}N_2(z,t) - (W_{01}^{\text{p}} + W_{01}^{\text{s}})N_0(z,t), \quad (1)$$

$$\frac{dN_1(z,t)}{dt} = (W_{01}^{\text{p}} + W_{01}^{\text{s}})N_0(z,t) + W_{21}N_2(z,t) - (W_{10} + W_{10}^{\text{p}} + W_{10}^{\text{s}})N_1(z,t) - 2W_{11}N_1(z,t)^2, \quad (2)$$

$$\frac{dN_2(z,t)}{dt} = W_{11}N_1(z,t)^2 - (W_{21} + W_{20})N_2(z,t), \quad (3)$$

where W_{ij} represents the spontaneous decay rate between energy level i and j, with the exception of W_{11}, which represents the homogeneous upconversion rate coefficient with units m^3s^{-1}. Thus, $W_{11}N_1$ is an excitation-dependent rate for homogeneous upconversion. The rates for pump and signal absorption, as well as stimulated emission, are

$$W_{01}^{\text{p}} = \frac{\Gamma_{\text{p}}\sigma_{01}^{\text{p}}\lambda_{\text{p}}}{hcA}P_{\text{p}}(z,t), \quad (4)$$

$$W_{10}^{\text{p}} = \frac{\Gamma_{\text{p}}\sigma_{10}^{\text{p}}\lambda_{\text{p}}}{hcA}P_{\text{p}}(z,t), \quad (5)$$

$$W_{01}^{\text{s}} = \frac{\Gamma_{\text{s}}\sigma_{01}^{\text{s}}\lambda_{\text{s}}}{hcA}P_{\text{s}}(z,t), \quad (6)$$

$$W_{10}^{\text{s}} = \frac{\Gamma_{\text{s}}\sigma_{10}^{\text{s}}\lambda_{\text{s}}}{hcA}P_{\text{s}}(z,t), \quad (7)$$

where $\Gamma_{\text{p/s}}$, $\sigma_{01}^{\text{p/s}}$, $\sigma_{10}^{\text{p/s}}$ and $\lambda_{\text{p/s}}$ are the power filling factor, absorption cross section, emission cross section and vacuum wavelength, respectively, for the pump and signal waves. h is Planck's constant, c is the speed of light in vacuum, and A is the fiber core cross section area. Lastly, $P_{\text{p/s}}$ is the optical power of the pump and signal waves. The parameter z represents the position on the optical axis of the fiber, which is divided into 100 fiber segments of equal length dz. The Ho doping concentration is assumed constant over a step-index fiber core, and the pump and signal

Optics EXPRESS

intensity profiles are approximated as Gaussian. The total number of single ions in the fiber is constant; thus, one of Eq. (1)–(3) can be replaced by $(1-2k)N_{\mathrm{Ho}} = N_0(z,t) + N_1(z,t) + N_2(z,t)$. The rate equations governing the population densities of ion pair states are

$$\frac{dN_3(z,t)}{dt} = (W_{10} + W_{10}^{\mathrm{p}} + W_{10}^{\mathrm{s}})N_4(z,t) + W_{20}N_6(z,t) - 2(W_{01}^{\mathrm{p}} + W_{01}^{\mathrm{s}})N_3(z,t), \tag{8}$$

$$\begin{aligned}\frac{dN_4(z,t)}{dt} = {} & 2(W_{01}^{\mathrm{p}} + W_{01}^{\mathrm{s}})N_3(z,t) + 2(W_{10} + W_{10}^{\mathrm{p}} + W_{10}^{\mathrm{s}})N_5(z,t) + W_{21}N_6(z,t) \\ & + W_{20}N_7(z,t) - (W_{01}^{\mathrm{p}} + W_{01}^{\mathrm{s}} + W_{10} + W_{10}^{\mathrm{p}} + W_{10}^{\mathrm{s}})N_4(z,t),\end{aligned} \tag{9}$$

$$\frac{dN_5(z,t)}{dt} = (W_{01}^{\mathrm{p}} + W_{01}^{\mathrm{s}})N_4(z,t) + W_{21}N_7(z,t) - 2(W_{10} + W_{10}^{\mathrm{p}} + W_{10}^{\mathrm{s}})N_5(z,t) - W_{\mathrm{pair}}N_5(z,t), \tag{10}$$

$$\frac{dN_6(z,t)}{dt} = W_{\mathrm{pair}}N_5(z,t) + (W_{10} + W_{10}^{\mathrm{p}} + W_{10}^{\mathrm{s}})N_7(z,t) - (W_{21} + W_{20} + W_{01}^{\mathrm{p}} + W_{01}^{\mathrm{s}})N_6(z,t), \tag{11}$$

$$\frac{dN_7(z,t)}{dt} = (W_{01}^{\mathrm{p}} + W_{01}^{\mathrm{s}})N_6(z,t) - (W_{10} + W_{10}^{\mathrm{p}} + W_{10}^{\mathrm{s}} + W_{20} + W_{21})N_7(z,t). \tag{12}$$

In these rate equations, it is assumed that only one energy transition can occur at a time for a given ion pair. Thus, the direct transition between two states involving the change of both ions is disregarded, the only exception being the upconversion process $N_5 \rightarrow N_6$. This assumption becomes valid in the limit of sufficient temporal resolution where the probability of two single-ion transitions taking place within a single simulation timestep becomes negligible. In our simulations, this condition was verified by reducing the timestep until the solution converged. The total number of ion pairs in the fiber is also constant; thus, one of Eq. (8)–(12) can be replaced by $kN_{\mathrm{Ho}} = N_3(z,t) + N_4(z,t) + N_5(z,t) + N_6(z,t) + N_7(z,t)$.

The optical power of the pump and signal waves evolve through the fiber as

$$\frac{dP_{\mathrm{p}}(z,t)}{dz} = \Gamma_{\mathrm{p}}\left[\sigma_{10}^{\mathrm{p}}N_{5_{\mathrm{I}_7}}(z,t) - \sigma_{01}^{\mathrm{p}}N_{5_{\mathrm{I}_8}}(z,t)\right]P_{\mathrm{p}}(z,t), \tag{13}$$

$$\frac{dP_{\mathrm{s}}(z,t)}{dz} = \Gamma_{\mathrm{s}}\left[\sigma_{10}^{\mathrm{s}}N_{5_{\mathrm{I}_7}}(z,t) - \sigma_{01}^{\mathrm{s}}N_{5_{\mathrm{I}_8}}(z,t)\right]P_{\mathrm{s}}(z,t). \tag{14}$$

Here, $N_{5_{\mathrm{I}_7}}$ is the population density of ions in the upper laser level and is given by $N_{5_{\mathrm{I}_7}} = N_1 + N_4 + 2N_5 + N_7$. $N_{5_{\mathrm{I}_8}}$ is the population density of ions in the ground state and is given by $N_{5_{\mathrm{I}_8}} = N_0 + 2N_3 + N_4 + N_6$. A few key assumptions of the model are worth emphasizing. Firstly, the single ions and paired ions are treated separately and do not interact with each other. Secondly, energy migration is not included. Thirdly, all single ions are treated collectively and are given a common upconversion rate coefficient.

4. Experimental setups

4.1. Time-resolved fluorescence measurements

We investigated the rapid kinetics of pair-induced quenching by measuring the intensity variation of the ~1.15 µm fluorescence stemming from the radiative transition $^5\mathrm{I}_6 \rightarrow {}^5\mathrm{I}_8$ indicated in Fig. 1, after a short pump pulse at 1.95 µm was sent into a Ho-doped fiber. The fluorescence build-up immediately following this pulse will correspond directly to the PIQ dynamics if we assume that the only way the Ho ions can become excited to $^5\mathrm{I}_6$ is through ETU from paired ions. For reference, this approach is entirely analogous to that used by Myslinski et al. [10] for erbium-doped fibers, only with our experiment adjusted to target corresponding energy levels of holmium.

The measurement setup is shown in Fig. 3. The 1.95 µm excitation source is a pulsed thulium-doped fiber amplifier, delivering 30 ns pulses at 100 Hz repetition rate and near square shape.

Optics EXPRESS

The amplifier can produce pulse energies up to 13 µJ. The pump source output fiber was spliced to the Ho-doped fiber under test (FUT), which in turn was spliced to a fiber connector pigtail. The output of the pigtail was collimated and passed through a long pass filter at 1000 nm and a short pass filter at 1550 nm to remove the potential residual pump and fluorescence stemming from unwanted energy transitions. The fluorescence was then focused onto an InGaAs avalanche photodiode (APD) (Excelitas LLAM-1550-R2AH) with a 50 MHz detection bandwidth, and the APD signal was sampled with a fast oscilloscope. An average of 2000 acquisitions was collected to improve the signal-to-noise ratio. Control measurements were done with an APD with considerably higher bandwidth (400 MHz), which verified that 50 MHz was sufficient to capture the full signal dynamics. The lower bandwidth APD was chosen because it offered lowered noise.

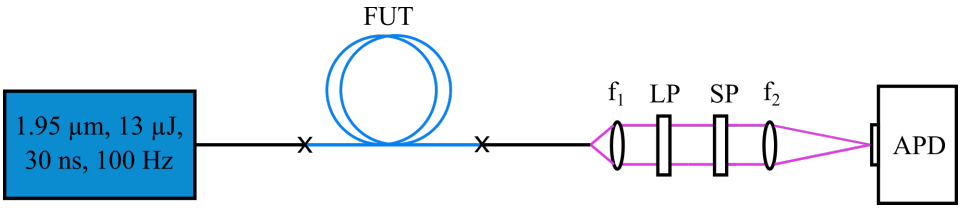

Fig. 3. Schematic of the measurement setup used in the $^5I_6$ fluorescence experiment. FUT: fiber under test, f: lenses, LP: long pass filter at 1000 nm, SP: short pass filter at 1550 nm, APD: avalanche photodiode.

4.1.1. Investigated holmium-doped fibers

In this study, we investigated twelve different Ho-doped fibers, labeled Fibers 1-12, sorted in order of increasing Ho doping concentration. Fibers 1-4 and 8-12 were provided by the Institute of Photonics and Electronics (Czech Republic), where Fiber 9 is described in Ref. [16] and the rest are described in Ref. [13]. These nine fibers correspond to SD1294 (1), NP1544 (2), NP1557 (3), SD1347 (4), NP1542 (8), NP1589 (9), SD1412 (10), SD1348 (11) and NP1558 (12) in the above references. Fibers 5-6 were provided by the Naval Research Laboratory (USA), where Fiber 5 is the fiber named 161129 described in Ref. [17]. Fiber 7 is the commercially available fiber IXF-HDF-PM-8-125 from Exail. The twelve fibers vary in Ho doping concentration in the wide range (1.1-10)×10^{25} ions/m^3. In Ref. [13,16], the concentrations of Fibers 1-4 and 8-12 were calculated from the small-signal absorption, using the formula $\alpha_{dB} = 10\log(e)\sigma_a N_{Ho}\Gamma$, where $\sigma_a = 2.95\times10^{-25}$ m^2 was used and Γ was for simplicity assumed to be one. For this reason, the concentrations of Fibers 5-7 were in this work calculated in the same way. All fibers had a core diameter of 10 µm, except for Fiber 7, which had a diameter of 8 µm. The fibers contain varying types and amounts of dopants, such as alumina (Al_2O_3), which are known to affect the probability of ion pair formation [13]. For reference, the investigated fibers have been shown to achieve slope efficiencies in the wide range of 41.8-83.1% in simple oscillator setups, where the lower than theoretical efficiencies are ascribed to Ho ion clustering and associated PIQ [13,16]. Furthermore, the slope efficiency was found to decrease with increasing Ho content and decreasing Al/Ho ratio.

The lengths of the fibers were chosen such that the test samples had about the same absorption of the pump pulses (~25 dB), being fairly short to reduce effects of re-absorption and re-emission while being long enough to get a sufficiently strong detector signal. A cut-back experiment was done with one of the fibers to verify that the measured fluorescence dynamics did not depend on the fiber length. The Ho doping concentrations, 1.95 µm small-signal absorption coefficients, Al/Ho ratio, and fiber lengths are summarized in Table 1 in Sec. 5.1.

Optics EXPRESS

Table 1. Summary of key fiber parameters as well as the determined pair lifetimes and effective $^5I_6$ lifetimes.

Fiber #	Ho^{3+} conc. ($\times 10^{25}$ m^{-3})	α_{dB} (dB/m)	Al/Ho	Length (cm)	τ_{pair} (ns)	Effective $^5I_6$ lifetime (μs)	Relative peak intensity
1	1.1	14.1	113.2	188	471	3.9	1.5
2	1.4	17.9	110.6	153	436	4.2	1.3
3	2.3	29.5	48.8	91	404	4.1	1
4	2.9	37.2	42.9	68	406	3.6	1.1
5	2.9	26	-	103	421	3.6	2.6
6	3.0	39	-	71	463	5.0	1.6
7	3.5	45	-	58	452	4.7	1.2
8	4.3	55.1	27.9	45	424	4.1	1.6
9	5.1	65.4	55	44	493	5.6	3.1
10	5.9	75.6	10.3	32	406	3.5	3.5
11	7.0	89.7	19.9	24	432	4.5	2.4
12	10	128	8.6	18	446	4.6	9.2

4.2. Non-saturable absorption measurements

Non-saturable absorption is one of the most commonly encountered manifestations of pair-induced quenching, and measuring its strength is a widely employed characterization method for quantifying the pair content in rare-earth-doped fibers. We measured the transmission through Fiber 12 as a function of input CW light at 1.95 μm in the interval 200 μW to 5 W. The measurements were done for three different lengths of the fiber. In order to avoid variations in splice loss, the output end of the Ho-fiber was spliced to a multi-mode fiber. Furthermore, to avoid measuring any generated amplified spontaneous emission (ASE), a spectral filter was used to separate the transmitted 1.95 μm light from ASE predominantly at wavelengths >1.95 μm.

4.3. Pair-induced quenching in a nanosecond-pulsed amplifier

To investigate the practical implications of pair-induced quenching on nanosecond-pulsed high-power holmium-doped fiber amplifiers, we developed the amplifier detailed in Fig. 4, aimed to study the dynamics associated with this phenomenon. The amplifier is designed as a master oscillator power amplifier (MOPA), where preamplified light from a 1.95 μm pump channel and a 2.1 μm signal channel was combined in a wavelength division multiplexer (WDM) and launched into a final power amplifier stage. Both the pump and signal channels operated in pulsed mode at 100 kHz with nearly square pulses of 20 ns duration. This power amplifier employs a so-called tandem setup with a Tm-doped fiber directly preceding a mode-matched Ho-doped fiber [2]. The Tm-doped fiber (Exail) had a core diameter of 20 μm, a cladding diameter of 300 μm, and a numerical aperture of 0.08. The Tm-doped fiber was cladding pumped at 793 nm, and provided gain predominantly for the 1.95 μm channel. This served as pump light in the Ho-doped fiber where the 2.1 μm signal was amplified. The average power of the 1.95 μm pump and 2.1 μm seed entering the Ho-doped fiber was 9.42 W and 630 mW, respectively. The temporal delay between the pump and seed pulses could be freely chosen in the experiment. We used this to probe the PIQ interaction by investigating the impact of varying delays on the amplifier conversion efficiency.

The Ho-doped fiber was the commercially available fiber IXF-HDF-PM-20-250 from Exail, which had a core diameter of 20 μm, cladding diameter of 250 μm, NA of 0.08, and a length of 1.2 m. This fiber has been demonstrated to achieve a relatively poor slope efficiency of 16% w.r.t. 1950 nm pump in an amplifier optimized for high pulse energy in 10 ns duration pulses [2]. Since

Optics EXPRESS

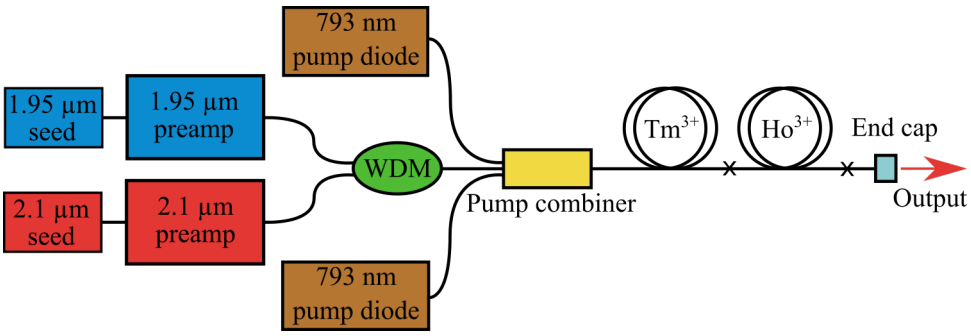

Fig. 4. Schematic of the holmium-doped fiber amplifier.

the performance of this fiber appears to be considerably affected by PIQ, this fiber was chosen as a good candidate for exploring the PIQ dynamics that are of interest in this work.

5. Results and discussion

5.1. Time-resolved fluorescence

Figure 5(a) shows the measured 1.15 µm fluorescence intensity after pulsed excitation for the selected holmium-doped fibers 3, 10, and 12. The excited pair lifetime is related to the rise time of the fluorescence signal. The intensity increases rapidly as excited Ho ion pairs undergo ETU. The signal reaches a maximum after ~1 µs, which is when the population increase of $^5I_6$ due to ETU and the rate of $^5I_6$ depopulation through spontaneous decay balance each other. A significant difference in peak fluorescence intensity for the three selected fibers can be observed, which we attribute to a difference in Ho pair content. The probability of ion pairs forming is expected to increase with doping concentration, and the observations in Fig. 5(a) are consistent with this; Table 1 shows that Fiber 12 has the highest doping concentration among the three fibers, and Fiber 3 has the lowest. The same general trend was seen for all the measured fibers, with some deviations from perfect correlation, which could, for instance, be explained by the various types and amounts of dopants, such as alumina, which affect ion pair formation [13]. The measured peak intensity for all the fibers relative to the lowest peak intensity fiber is listed in Table 1.

To validate that the temporal evolution of the fluorescence intensity was independent of the fiber length, measurements were done on three different lengths of Fiber 12. Figure 5(b) shows the resulting fluorescence for the lengths 175 mm, 85 mm and 40 mm. The highest peak intensity is measured for the 85 mm fiber. We explain this observation from incomplete pump absorption for the shortest fiber and signal attenuation by re-absorption in the longest fiber. Nevertheless, when the signals are scaled to the same peak intensity, as shown in Fig. 5(c), the fluorescence intensities for the three lengths are indistinguishable.

Measurements of Fiber 12 were also done using two different pulse energies, 3.1 µJ and 13 µJ, to look for any potential dependence of fluorescence dynamics on the degree of excitation. Figure 5(d) shows the fluorescence curves for these pulse energies. The high-energy pulses excite more Ho ion pairs; thus, the emitted fluorescence is more intense. However, the fluorescence dynamics appear identical when the signals are scaled to the same peak intensity, as Fig. 5(e) shows. A core difference between homogeneous upconversion and PIQ is that the homogeneous upconversion rate increases with the degree of excitation, whereas the PIQ rate is independent.

Optics EXPRESS

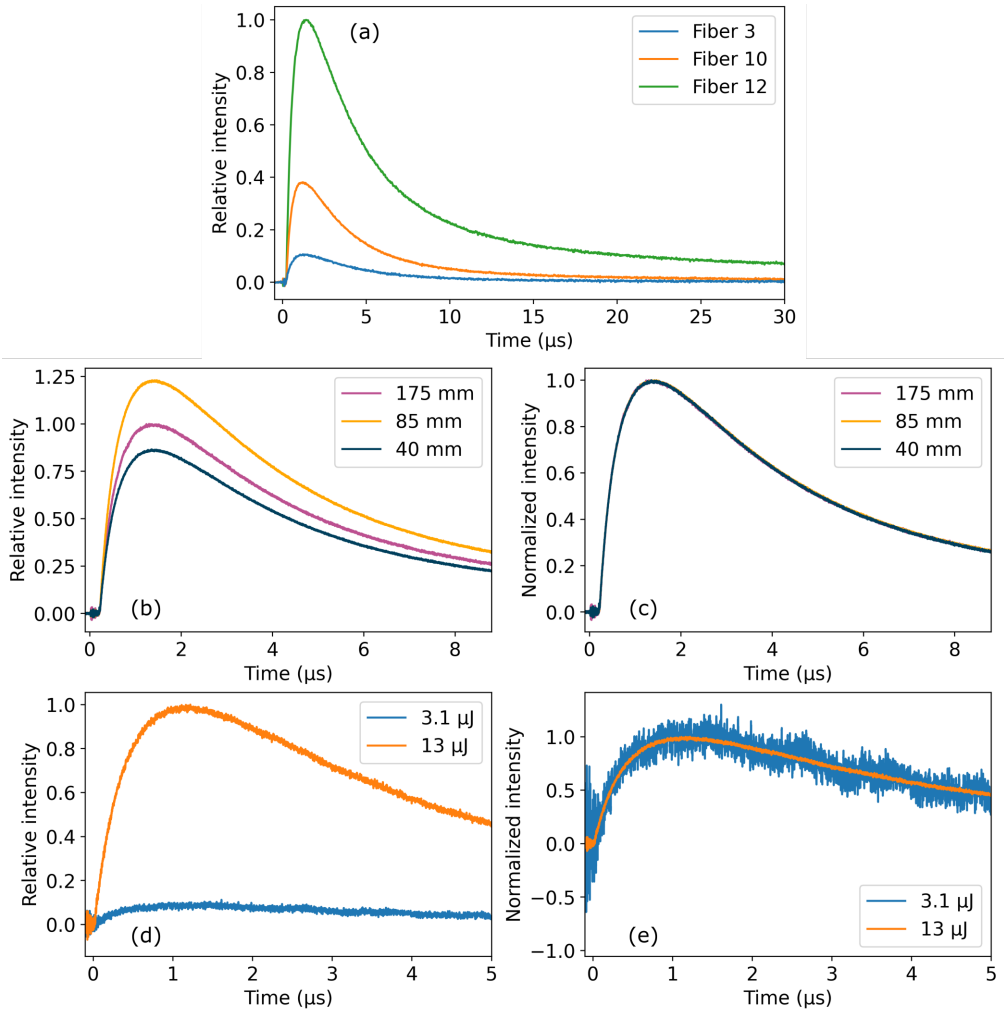

Fig. 5. (a) Measured 1.15 μm fluorescence intensity from Fibers 3, 10 and 12 after the 30 ns 1950 nm pump pulse. (b) Measured fluorescence intensity for three lengths of Fiber 12, relative to the peak intensity of the 175 mm measurement. (c) The fluorescence measurements from (b) normalized. (d) Fluorescence intensity measurements from Fiber 12 for two different excitation pulse energies; 3.1 μJ and 13 μJ, relative to the peak intensity of the 13 μJ measurement. (e) The fluorescence measurements from (d) normalized.

Optics EXPRESS

Thus, our result from Fig. 5(e) strongly indicates that the measured fluorescence primarily stems from ions that underwent PIQ.

In simple terms, the rate of PIQ (i.e., the excited pair lifetime) corresponds to the rise time of the fluorescence signals in Fig. 5(a). However, because the fluorescence signals decay at a slower yet non-negligible rate compared to the rise time, one cannot simply take the $1/e$-crossing points of the curves in Fig. 5(a) to be the pair lifetime. For reference, this contrasts the study of PIQ in erbium-doped fibers by Myslinski et al. [10], where such simple analysis was possible because the Er pair lifetime was measured to be 50 ns, and the lifetime of the Er state $^4I_{11/2}$ (analogous to $^5I_6$ in Ho) was orders of magnitude longer (3-7 µs for the tested fibers). In this work, we determine instead the lifetime of excited Ho ion pairs by fitting the numerical model presented in Sec. 3. to the measured fluorescence curves. We simulate a single 30 ns super-Gaussian pump pulse at 1.95 µm wavelength and 13 µJ pulse energy, propagating through the fiber. Thus, the optical power at the signal wavelength in Eq. (14) is zero ($P_s(z,t) = 0$). Consequently, the rates for absorption and stimulated emission at the signal wavelength are also zero ($W^s_{01} = 0$ and $W^s_{10} = 0$). We track the time variation of the total population of ions excited to $^5I_6$ in the fiber, which will be proportional to the fluorescence intensity. As Fig. 5(e) indicates, and as we also confirmed through varying the homogeneous upconversion coefficient W_{11} in our simulations, we could neglect the contributions from HUC in the fitting. Therefore, we set $W_{11} = 0$ for the rest of this analysis.

Figure 6 shows the measured 1.15 µm fluorescence evolution from Fiber 6 during the first 5 µs after the excitation pulse, as well as the result of a simulation. In this simulation, the $^5I_6$ lifetime is used as a variable parameter along with the pair lifetime to best fit the experimental results. The parameter values that provided the best fit are $\tau_{^5I_6} = 5.0$ µs and $\tau_{\text{pair}} = 463$ ns. This "effective" $^5I_6$ lifetime is introduced heuristically to correct for the slow decay of the fluorescence signal, compared to the published value of 1.4 µs [12]. We suspect that the discrepancy can have several explanations where likely contributors include effects of energy transfer mechanisms that are not accounted for in the numerical model. We anticipate, for example, that energy migration [12] could be one mechanism that would allow pairs to become excited long after pulse excitation. Additionally, ETU in larger clusters may occur over a prolonged time since ions relaxing from $^5I_6$ to $^5I_7$ can undergo additional ETU. The effective $^5I_6$ lifetime thus approximates the combined effects from such contributing mechanisms. It is noted that variations in the effective $^5I_6$ lifetime mainly affect the decaying parts of the simulated fluorescence evolution, whereas the pair lifetime that is of interest in this work is predominantly determined from the rising parts of the curves.

The excited pair lifetimes for all twelve fibers were determined by finding the simulation parameters for pair lifetime and effective $^5I_6$ lifetime that provided the least square error between the simulation and experimental data. The resulting pair lifetimes are shown in Table 1, together with the corresponding effective $^5I_6$ lifetimes. The pair lifetime varied in the range of 404-493 ns with an average of 438 ns. This narrow span (±10.5%) of lifetimes supports the picture of PIQ, where ETU within pairs is an isolated process where the rate is not significantly affected by parameters such as doping concentration and doping chemistry. Again, this is in contrast to homogeneous ETU, which strongly depends on the doping concentration. These findings are analogous to the observations made by Myslinski et al. of PIQ in Er-doped fibers [10]. However, the measured excited pair lifetime of Ho is notably almost an order of magnitude longer than the Er pair lifetime of 50 ns. In the two following sections, we will see that the long lifetime we have measured for excited Ho pairs has important implications for our understanding of phenomena associated with PIQ, such as non-saturable absorption and its relevance to the operation of nanosecond-pulsed fiber amplifiers.

Optics EXPRESS

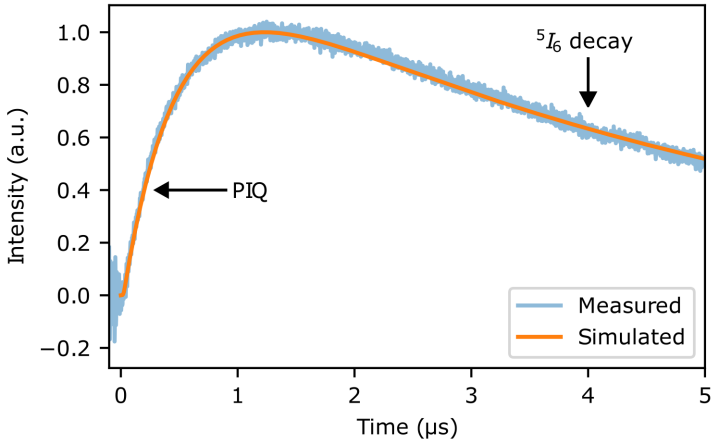

Fig. 6. The measured 1.15 μm fluorescence from Fiber 6 and the result of a simulation with best-fit parameters: 5.0 μs for the effective $^5I_6$ lifetime and 463 ns for the pair lifetime.

5.2. Non-saturable absorption

A simple and commonly used method for determining the pair content of a rare-earth-doped fiber is by measuring the strength of non-saturable absorption (NSA) [2,6,7,11]. The presence of pairs gives rise to NSA since the rapid PIQ process prevents more than one ion in a cluster from being excited at any given time. The fraction of ions residing in pairs is with this method determined through [11]

$$2k = \frac{\alpha_{\mathrm{ns}}}{\alpha_{\mathrm{ss}}} \cdot \frac{2\sigma_{\mathrm{a}} + \sigma_{\mathrm{e}}}{\sigma_{\mathrm{a}}}, \tag{15}$$

where α_{ns} is the measured non-saturable absorption, α_{ss} is the small-signal absorption, and σ_{a} and σ_{e} are the absorption and emission cross sections at the measurement wavelength. This strategy for determining pair content is notably appealing since it only requires knowledge of a few spectroscopic parameters that are all relatively easy to measure. However, a key assumption of the method is that there exists a power interval where the absorption caused by single ions is fully saturated, while there is still a negligible population of doubly-excited pairs. Given the relatively long Ho pair lifetime we have found in Sec. 5.1, it is natural to question the validity of this assumption.

Figure 7(a) shows the measured transmission of 1950 nm light through different lengths of Fiber 12, as well as results from a simulation where the measured excited pair lifetime of 446 ns was implemented. Other parameters used in this simulation are summarized in Appendix A. If Eq. (15) is valid, it is expected that the transmission will, at high power levels, reach a plateau somewhere below 100% when the absorption by single ions would be fully saturated. However, Fig. 7(a) shows that no such plateau is reached in either the measurements or in the simulations that could be done at high powers. We attribute this to the long excited pair lifetime that permits the presence of doubly-excited pairs at an intensity lower than that required for complete saturation of single ion absorption. Figure 7(b) illustrates this point directly by showing the simulated populations of excited single ions and doubly-excited pairs as a function of power.

Measurements of NSA have previously been used to estimate the pair content of Ho-doped fibers [2,6,7], where pump intensities corresponding to about 1-3 W in our experiment were used. There is a plateauing tendency evident in Fig. 7(a) around this power level, which indeed corresponds to saturation of single ion absorption. However, α_{ns} is not really a well-defined parameter without a clear plateau in the transmission curves. Furthermore, in the transmission curves we measured from the lower Ho concentration fibers, which have a lower expected

Optics EXPRESS

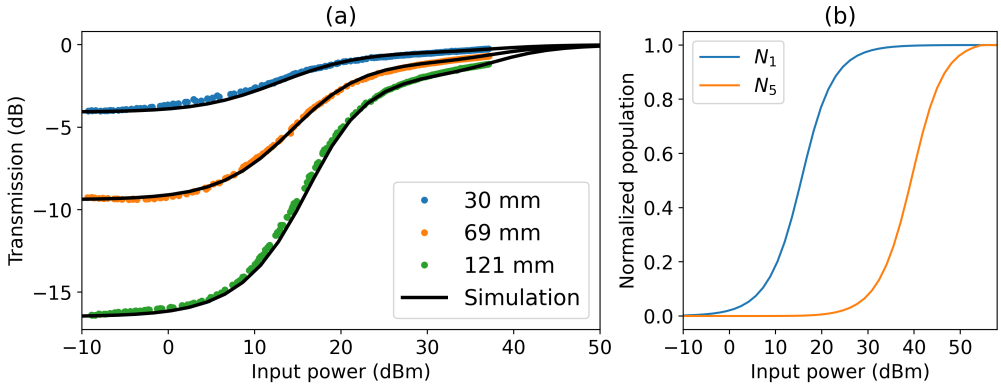

Fig. 7. (a) The measured transmission of 1950 nm light through different lengths of Fiber 12. (b) The simulated population of single ions excited to $^5I_7$ (N_1) and population of doubly-excited pairs (N_5) for a range of input powers. A population of 1 represents the population reached when the absorption is fully saturated.

pair fraction, the plateau was even less noticeable. From this, we conclude that simple NSA measurements are not a robust method for determining pair content in Ho-doped fibers, contrary to previous assumptions. Accurate determination of pair content likely requires comparison with a complete rate equation model.

5.3. Impact of PIQ on a nanosecond-pulsed amplifier

We studied the impact of PIQ on a nanosecond-pulsed holmium-doped fiber amplifier by measuring the optical-to-optical conversion efficiency obtained when varying the temporal delay between pump and seed signal pulses. Figure 8(a) illustrates how the pulse trains look for three different pump-seed delays. It is noted that delays corresponding to any direct overlap of the 20 ns pump and signal pulses were avoided in the experiment because this would result in unwanted Raman conversion from the pump to the signal. The measured efficiency w.r.t. launched 1.95 µm pump of the amplifier described in Sec. 4.3 is shown in Fig. 8(b) as a function of the pump-seed delay. The figure shows that the efficiency decreases from 50.5%, with the shortest delay where the signal pulses arrive immediately after the pump pulses, to 43.4% for the longest delay where the signal pulses arrive just before the next pump pulses. The highest efficiency corresponds to an output power of 5.4 W at 2.1 µm, and the lowest efficiency corresponds to a power of 4.7 W. The efficiency is notably seen to decrease rapidly for increasing delay at a timescale comparable to the pair lifetime of 0.4-0.5 µs that was measured in Sec. 5.1. This initial drop is therefore consistent with the idea that PIQ is responsible for reducing the upper-state population in the time between the pump and seed pulses. For delays above ~2 µs (i.e., a few pair lifetimes), essentially all pairs will have undergone PIQ, and the efficiency curve shows a weakly declining trend that we attribute to the depopulation of the upper laser level through homogeneous upconversion.

The efficiency of the amplifier was also measured when CW pumping was utilized instead of pulsed pumping, but the seed was pulsed as before. For comparison, the CW pump power was set to the same average power as in the pulsed pump experiments. As shown in Fig. 8(b), this resulted in an efficiency of 32.7%, much lower than with pulsed pumping even with the longest delay. Interestingly, switching from CW pumping to pulsed pumping had a significantly larger impact on efficiency than varying the delay from the longest to the shortest with pulsed pumping. This observation can be fully explained by the PIQ effect: when CW-pumped, ion pairs excited early in the period will quickly decay through PIQ. Thus, any given ion pair can be re-excited followed by PIQ several times during a single period. In contrast, by pumping with short pulses

Optics EXPRESS

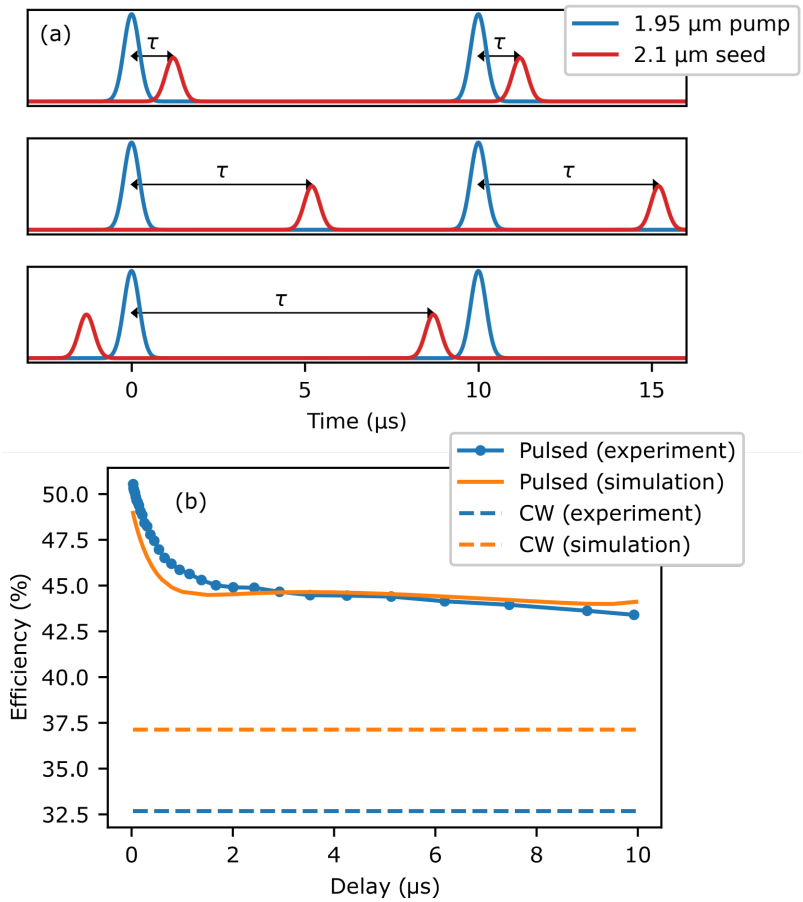

Fig. 8. (a) Illustration of the varying delay between the 1.95 µm pump and 2.1 µm seed pulses. (b) The measured and simulated conversion efficiency w.r.t launched 1.95 µm pump of a pulsed holmium-doped fiber amplifier for different delays between the 1.95 µm pump pulses and 2.1 µm seed pulses, as well as the efficiency of the same amplifier when it is CW-pumped.

compared to the pair lifetime, any given pair can only be excited and undergo PIQ once in a single period. Thus, much less energy is wasted when the amplifier is pulse-pumped compared to CW-pumped.

Figure 8(b) also shows the results of numerical simulations of an equivalent Ho-doped fiber amplifier for pulsed pumping with different delays, as well as simulations of CW pumping. In these simulations, the pair lifetime was chosen to be 470 ns, which gave reasonable agreement with the rapid decay in efficiency measured experimentally for short delays. Additionally, a pair content of $2k = 20\%$ was chosen. As Fig. 8(b) shows, the simulation of the pulsed amplifier fits reasonably well with the experimental results, which suggests that the numerical model is successful in capturing the important dynamic aspects of PIQ. The simulated efficiency is seen to be significantly lower when the amplifier is CW-pumped. This agrees qualitatively with the experimental results; however, the model underestimates the magnitude of this difference. This discrepancy might be caused by energy transfer mechanisms that are not included in the numerical model. For instance, energy migration can transport excitation between ions until an ion pair is reached, increasing the effective impact of PIQ for a given pair content.

Optics EXPRESS

6. Conclusion

We have investigated the fast kinetics of pair-induced quenching in holmium-doped optical fibers. The lifetime of excited Ho ion pairs was measured to be 0.4-0.5 µs for the twelve studied fibers, which was found through time-resolved fluorescence measurements and a numerical model that takes into account the fast but finite rate of PIQ. The estimated excited pair lifetime was found to vary little among the fibers (±10.5%), which indicates that the upconversion process within pairs is an isolated process with dynamics that are largely independent of composition and doping concentration in the core. Furthermore, we studied the commonly encountered manifestation of PIQ called non-saturable absorption, frequently used to measure the pair content of fibers. We showed that the accuracy of this measurement technique becomes questionable due to the relatively long excited pair lifetime of Ho ion pairs. Finally, the impact of PIQ on a nanosecond-pulsed fiber amplifier was investigated experimentally and numerically. We found that by utilizing short pump pulses compared to the pair lifetime, the efficiency of the amplifier could be improved to 50.5% compared to 32.7% when continuous wave pumping was used. The numerical model developed in this work was successful in recreating the experimental results and is therefore expected to become a valuable tool for modeling pulsed Ho-doped fiber amplifiers with pulse widths comparable to or shorter than the excited pair lifetime.

Appendix. Simulation input parameters

The numerical simulations in this work requires several input parameters. Parameters that are common for all simulations and have not been specified previously are: $\sigma_{01}^{p} = 2.95\times10^{-25}$ m^2, which is obtained from Ref. [13], $\sigma_{10}^{p} = 2.43\times10^{-25}$ m^2, $\sigma_{01}^{s} = 0.194\times10^{-25}$ m^2, $\sigma_{01}^{s} = 1.18\times10^{-25}$ m^2, $W_{20} = 72.25\text{s}^{-1}$ and $W_{21} = 7.14E5\text{s}^{-1}$, which are obtained from Ref. [6]. The rate W_{10} is calculated from the $^5I_7$ fluorescent lifetime, which can be found for Fibers 1-4, 8 and 10-12 in Ref. [13] and for Fiber 9 in Ref. [16]. The fiber parameters that have not been mentioned and are specific to these nine fibers can also be obtained from Ref. [13,16]. For Fibers 5-7 and the fiber used in the amplifier, a $^5I_7$ lifetime of 1 ms was assumed. The numerical aperture of Fibers 5 and 6 was 0.18 and 0.174, respectively. For the fiber used in the amplifier simulation, a $^5I_6$ lifetime of 1.4 µs [12] was assumed and a doping concentration of $N_{Ho} = 5.62\times10^{25}$ m^{-3}, calculated from the pump absorption coefficient was used. The rate coefficient of homogeneous upconversion was set to $W_{11} = 4.0\times10^{-23}$ m^{3}s^{-1} [6].

Acknowledgments. We thank Pavel Peterka from the Institute of Photonics and Electronics (UFE) and Colin Baker from the Naval Research Laboratory (NRL) for kindly providing holmium-doped optical fibers studied in this work.

Disclosures. The authors declare no conflicts of interest.

Data availability. Data underlying the results presented in this paper are not publicly available at this time but may be obtained from the authors upon reasonable request.

References

1. A. Hemming, N. Simakov, J. Haub, *et al.*, "A review of recent progress in holmium-doped silica fibre sources," Opt. Fiber Technol. **20**(6), 621–630 (2014).
2. L. G. Holmen and H. Fonnum, "Holmium-doped fiber amplifier for pumping a $ZnGeP_2$ optical parametric oscillator," Opt. Express **29**(6), 8477–8489 (2021).
3. A. Hemming, N. Simakov, M. Oermann, *et al.*, "Record efficiency of a holmium-doped silica fibre laser," in *2016 Conference on Lasers and Electro-Optics (CLEO)*, (IEEE, 2016), pp. 1–2.
4. W. Yao, C. Shen, Z. Shao, *et al.*, "High-power nanosecond pulse generation from an integrated Tm–Ho fiber MOPA over 2.1 µm," Opt. Express **26**(7), 8841–8848 (2018).
5. J. Wang, D. Yeom, N. Simakov, *et al.*, "Numerical modeling of in-band pumped Ho-doped silica fiber lasers," J. Lightwave Technol. **36**(24), 5863–5880 (2018).
6. J. Wang, N. Bae, S. B. Lee, *et al.*, "Effects of ion clustering and excited state absorption on the performance of Ho-doped fiber lasers," Opt. Express **27**(10), 14283–14297 (2019).
7. J. L. Gouët, F. Gustave, P. Bourdon, *et al.*, "Realization and simulation of high-power holmium doped fiber lasers for long-range transmission," Opt. Express **28**(15), 22307–22320 (2020).

Optics EXPRESS

8. H. Masuda, A. Takada, and K. Aida, "Modeling the gain degradation of high concentration erbium-doped fiber amplifiers by introducing inhomogeneous cooperative up-conversion," J. Lightwave Technol. **10**(12), 1789–1799 (1992).
9. E. Delevaque, T. Georges, M. Monerie, *et al.*, "Modeling of pair-induced quenching in erbium-doped silicate fibers," IEEE Photonics Technol. Lett. **5**(1), 73–75 (1993).
10. P. Myslinski, J. Fraser, and J. Chrostowski, "Nanosecond kinetics of upconversion process in EDF and its effect on EDFA performance," in *Optical Amplifiers and Their Applications*, (Optica Publishing Group, 1995), p. ThE3.
11. P. Myslinski, D. Nguyen, and J. Chrostowski, "Effects of concentration on the performance of erbium-doped fiber amplifiers," J. Lightwave Technol. **15**(1), 112–120 (1997).
12. S. D. Jackson, "The spectroscopic and energy transfer characteristics of the rare earth ions used for silicate glass fibre lasers operating in the shortwave infrared," Laser Photonics Rev. **3**(5), 466–482 (2009).
13. M. Kamrádek, I. Kašík, J. Aubrecht, *et al.*, "Nanoparticle and solution doping for efficient holmium fiber lasers," IEEE Photonics J. **11**(5), 1–10 (2019).
14. P. F. Wysocki, J. L. Wagener, M. J. F. Digonnet, *et al.*, "Evidence and modeling of paired ions and other loss mechanisms in erbium-doped silica fibers," in *Fiber Laser Sources and Amplifiers IV*, vol. 1789 M. J. F. Digonnet and E. Snitzer, eds., International Society for Optics and Photonics (SPIE, 1993), pp. 66–79.
15. J. Nilsson, B. Jaskorzynska, and P. Blixt, "Implications of pair-induced quenching for erbium-doped fiber amplifiers," in *Optical Amplifiers and Their Applications*, (Optica Publishing Group, 1993), p. MD19.
16. M. Kamrádek, J. Aubrecht, M. Jelínek, *et al.*, "Holmium-doped fibers for efficient fiber lasers at 2100 nm," in *Mid-Infrared Coherent Sources*, (Optical Society of America, 2020), pp. MTh3C–5.
17. C. C. Baker, E. J. Friebele, A. A. Burdett, *et al.*, "Nanoparticle doping for high power fiber lasers at eye-safer wavelengths," Opt. Express **25**(12), 13903–13915 (2017).